Removal of background signals from fluorescence thermometry measurements in PDMS microchannels using fluorescence lifetime imaging

Tom Robinson,[ae] Yolanda Schaerli,[b] Robert Wootton,[b] Florian Hollfelder,[b] Christopher Dunsby,[c] Geoff Baldwin,[d] Mark Neil,[c] Paul French*[c] and Andrew deMello*[e]

Received 6th July 2009, Accepted 25th August 2009
First published as an Advance Article on the web 24th September 2009
DOI: 10.1039/b913293g

We report a method for removing unwanted contributions to fluorescence signals from dyes absorbed in polydimethylsiloxane (PDMS) using fluorescence lifetime imaging microscopy (FLIM). By analysing experimental fluorescence decays using a bi-exponential decay model, we are able to discriminate between emission originating from dye molecules in free solution and those absorbed within the PDMS substrate. Simple image processing allows the unwanted background signal to be removed and thus enables a more accurate assessment of temperature. The efficacy of the approach is demonstrated by measuring temperature changes within a droplet-based PCR device.

Introduction

Microfluidic applications such as PCR[1] or nanoparticle synthesis[2] rely on precise temperature control. To ensure maintenance of a defined thermal environment, accurate temperature measurements must be made, however this can be problematic due to the small volumes associated with microfluidic channels. While thermocouples may be inserted into device substrates, they provide insufficient spatial resolution.[3] NMR thermometry and other methods also suffer from low spatial resolution.[4] A more effective approach is to use fluorescence microscopy to monitor fluorescence from a small molecule fluorophore (whose intensity is dependent on temperature) dissolved in the fluid flowing through the device. This approach has been shown to deliver high spatial resolution but requires the acquisition of an image at a known baseline temperature prior to each experiment (for normalisation purposes).[5] This method is also compromised by background signal from dye absorbed into the PDMS channel walls.

A large proportion of microfluidic devices described in the literature are now made from PDMS, which is known to absorb hydrophobic molecules such as rhodamine B. The increasing amount of rhodamine B absorbed over time provides a significant background signal, which reports different thermal characteristics to the aqueous solution, making fluorescence-based temperature measurements imprecise. The problem is exacerbated at higher fluidic temperatures as the rate of absorption into the PDMS increases, especially if the PDMS is also heated. Glass microfluidic devices do not absorb dyes and are therefore preferable for this application; however they take longer to manufacture and are more expensive. Therefore it is desirable to find a means of minimising the background fluorescence signal due to absorption in the PDMS substrate.

It should be noted that a number of approaches to reduce absorption into PDMS have been proposed. For example the surface of the PDMS walls within a channel can be oxidised with an oxygen plasma prior to experiment. This process does reduce absorption but only for a few hours.[6] Alternatively a surfactant can be introduced into the buffer to dynamically coat the PDMS walls[7] or the PDMS can be coated with a polytetrafluoroethylene (PTFE) layer prior to use.[8] Absorption is inherently reduced in segmented flow systems as the sample is contained in an aqueous droplet[9,10] but it is not completely eliminated as some dye will be transferred *via* the oil phase, especially in mineral oil systems.[11] A method recently reported in this journal involves photobleaching both the sample and substrate before a measurement is made.[12] Unfortunately, while this does remove the background signal on a short timescale, further dye absorption is possible during the measurement process and more worryingly the high power light source used to photobleach the sample may result in local heating of the device, which will lead to inaccuracies in measured temperatures. Indeed, whilst it is evident that the above methods may be partially effective in some situations, they do not completely eliminate absorption artefacts and thus a more general solution is required.

Herein we describe a direct method for removing unwanted fluorescence due to dyes absorbed in PDMS substrates using FLIM. Importantly, we have previously shown that FLIM is effective in precisely mapping temperature variations in microchannels.[13] It is a ratiometric technique that does not require calibration prior to each experiment; with the variation of the fluorescence lifetime as a function temperature being measured once or extracted from the literature.[14] In the current system, the fluorescence lifetime of rhodamine B is significantly longer when absorbed in PDMS than when dissolved in water. Accordingly, fitting measured fluorescence decay curves to a bi-exponential model can be used to directly discriminate between absorbed and

[a]*Chemical Biology Centre, Imperial College London, Exhibition Road, London, SW7 2AZ, UK*
[b]*Department of Biochemistry, University of Cambridge, 80 Tennis Court Road, Cambridge, CB2 1GA, UK*
[c]*Photonics Group, Department of Physics, Exhibition Road, London, SW7 2AZ, UK. E-mail: paul.french@imperial.ac.uk*
[d]*Division of Molecular Biosciences, Exhibition Road, London, SW7 2AZ, UK*
[e]*Department of Chemistry, Exhibition Road, London, SW7 2AZ, UK. E-mail: a.demello@imperial.ac.uk*

free dye. In turn, the fluidic temperature can then be extracted from the aqueous dye lifetime without interference from the absorbed dye. We demonstrate this approach using a continuous-flow droplet-based PCR device and show that it is possible to extract precise fluidic temperature changes even with a large amount of rhodamine B absorbed into the PDMS channel walls. To our knowledge this is the first method that completely overcomes the issue of signal pollution in PDMS devices.

Experimental

FLIM images were acquired using a confocal microscope (SP5, Leica Microsystems) with time-correlated single photon counting (TCSPC) detection (SPC-830, Becker & Hickl). 530 nm excitation light was produced by filtering the supercontinuum generated by pumping a photonic crystal fibre with 120 fs pulses at 800 nm from a Ti:Sapphire laser (Mai Tai, Spectra-Physics) using a mirror slit arrangement.[15] The sample was illuminated through a 0.3 NA 10× air objective (Leica Microsystems) to give a large field of view and fluorescence emission (550–600 nm) was collected through the same objective, filtered internally in the confocal microscope and detected with a photon-counting photomultiplier tube. A schematic of the setup is shown in Fig. 1. A reference time signal was provided to the TCSPC card from a photodiode illuminated by a small part of the excitation beam.

FLIM images were analysed using SPCImage (Becker & Hickl) with the required fluorescence decay model convolved with the instrument response function (IRF) to provide an accurate assessment of the molecular decay. Subsequent temperature maps were calculated from a calibration curve (see ref. 14 for details of the method) using a MatLab program written in-house. Typical image acquisition times were 5 minutes to ensure sufficient signal-to-noise ratios for analysis using a bi-exponential model.

PDMS microfluidic devices were fabricated using conventional soft lithographic methods as described elsewhere.[16] Channels were 75 μm deep and 200–500 μm wide. The aqueous phase used in all experiments was 500 μM rhodamine B in 50 mM Tris/HCl at pH 6.8 and the oil phase was 3% ABIL EM 90 (w/w) in mineral oil. A volumetric flow rate of 2 μl min^{-1} was used and the device was heated as described by Schaerli *et al.*[14]

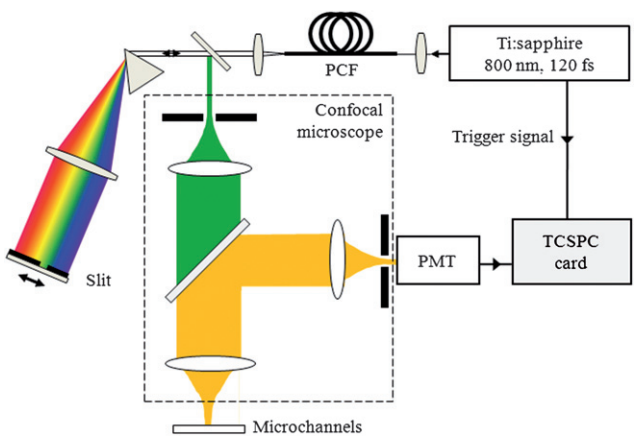

Fig. 1 Experimental setup showing supercontinuum generation, the confocal microscope and TCSPC detection.

Results and discussion

As described previously, the fluorescence lifetime of rhodamine B is dependent on both its temperature and the solvent in which it is dissolved. In a sample with populations of dye in water and in PDMS, it is therefore possible to resolve two separate fluorescence decay components by fitting a bi-exponential model to the recorded fluorescence decay for each pixel. The shorter lifetime component originates from the dye in the aqueous phase and its lifetime value is used to determine the local temperature. Crucially, this is possible even in the presence of a background signal (the longer lifetime component) from dye absorbed into PDMS.

Fig. 2a shows a fluorescence intensity image of a region in a microfluidic device heated to 90 °C through which aqueous dye solution has been flowing for 10 minutes. Region A is within the PDMS wall and region B is in the channel. During this period dye has been absorbed into the PDMS and fluorescence can be seen in both regions. The pixels from region A were then binned and analysed using a single exponential decay model as shown in eqn (1) where $I(t)$ is the intensity at time t, I_0 is the intensity at $t = 0$, and τ is the fluorescence lifetime.

$$I(t) = I_0 e\left(-\frac{t}{\tau}\right) \quad (1)$$

The resulting fit and residuals are shown in Fig. 2c. In this region dye is only present in PDMS and hence the fluorescence is well fitted by a single exponential decay yielding a lifetime of 3.1 ns. Without binning the mean lifetime was 3.1 ± 0.5 ns over all the pixels in region A. In contrast, region B contains signal from both aqueous dye and that absorbed in PDMS. Accordingly, the binned pixels from region B were fitted to a bi-exponential model, shown in eqn (2) where A_1 and A_2 are pre-exponentials factors associated with lifetime components τ_1 and τ_2 respectively.

$$I(t) = I_0\left(A_1 e^{\left(-\frac{t}{\tau_1}\right)} + A_2 e^{\left(-\frac{t}{\tau_2}\right)}\right) \quad (2)$$

The fitted decay and residuals are shown in Fig. 2d. It is clear that two distinct populations of dye are present with the bi-exponential fit yielding a longer lifetime component of 3.2 ns (equal to that of the dye in PDMS alone with a mean lifetime 3.2 ± 0.4 ns over all the pixels) and a shorter component of 0.3 ns (representative of the dye in aqueous solution with a mean lifetime of 0.3 ± 0.1 ns over all the pixels). A similar image was then acquired after 40 minutes of operation (Fig. 2b) and the pixels from region B were again binned and fitted to a bi-exponential model, as shown in Fig. 2e. This produced lifetime components of 3.2 ns and 0.3 ns (with mean lifetimes of 3.1 ± 0.2 ns and 0.2 ± 0.1 ns). As expected, more of the dye was absorbed into the PDMS, which is evident when comparing Fig. 2a and 2b. Comparing the fits in Fig. 2e and 2d reveals an increase in the contribution from the long lifetime component (associated with dye in PDMS) from 64 ± 5% to 77 ± 3%, as calculated by eqn (3).[17] This corresponds to an 88% increase in the number of rhodamine B molecules absorbed over a 30 minute period.

$$f_2 = \frac{A_2\tau_2^2}{A_1\tau_1 + A_2\tau_2} \quad (3)$$

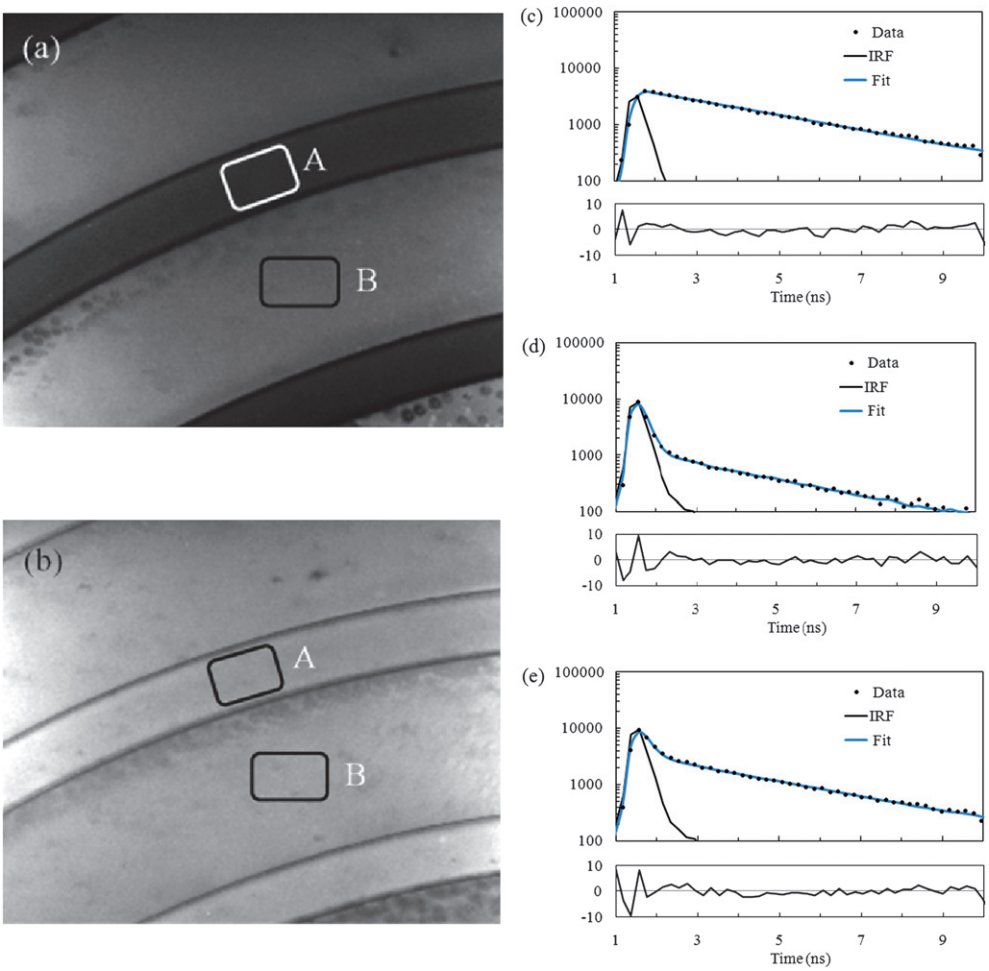

Fig. 2 Fluorescence intensity images and decay curves for the microfluidic device. Region A is within the PDMS wall and region B is inside the channel. (a) Intensity image after 10 minutes of operation. (b) Intensity image of the same region after 40 minutes. (c) Fluorescence decay, single exponential fit and residuals from region A after 10 minutes ($\chi^2 = 1.31$). (d) Fluorescence decay, bi-exponential fit and residuals from region B after 10 minutes ($\chi^2 = 1.55$). (e) Fluorescence decay, bi-exponential fit and residuals from region B after 40 minutes ($\chi^2 = 1.21$).

Thus, despite the large amount of dye absorbed into the PDMS and the correspondingly large background fluorescence signal (which exceeds that of the aqueous dye signal), the time-resolved fluorescence measurement is able to distinguish the two populations and provide an accurate estimate of the channel temperature of 90 ± 5 °C.

To further demonstrate the efficacy of the technique we applied it to a new device using oil and water to create a segmented (or droplet) flow. A high-temperature zone for DNA denaturation and an annealing/extension region in the PCR device were imaged and the observed fluorescence signals fitted to a bi-exponential model. The average lifetime, $\bar{\tau}$, was calculated using eqn (4) and is displayed in the false colour lifetime maps in Fig. 3a.

$$\bar{\tau} = \frac{A_1\tau_1^2 + A_2\tau_2^2}{A_1\tau_1 + A_2\tau_2} \quad (4)$$

Inspection of the images of the denaturation and annealing/extension regions indicates that the longer lifetime value (of the absorbed dye) is approximately 3.1 ± 0.2 ns in both regions whilst the lifetime value of the aqueous dye changes from 0.30 ± 0.01 ns in the denaturation zone to 0.72 ± 0.02 ns in the annealing/extension region. Importantly, the thermal change does not affect the PDMS-absorbed lifetime component since the mobility of the fluorophore is highly restricted inside the PDMS matrix and thus non-radiative relaxation is less favoured than when in the fluid state. By plotting *only* the short lifetime component, it is possible to remove the unwanted background signal and the resulting temperature maps are shown in Fig. 3b. For comparison, if only a single exponential decay model is used to fit the raw data then the images in Fig. 3c are obtained. It can be seen that these suggest an 'artificially' lower temperature due to the systematic error arising from the background fluorescence from dye in the PDMS, illustrating the improvement in accuracy provided by the use of a bi-exponential fit. The remaining error in the fitted lifetimes scaled inversely with the square-root of the pixel binning, which is consistent with random noise on the data. This could be significantly improved by increasing the acquisition time to achieve a better signal-to-noise ratio.

Crucially, these data show that by applying a bi-exponential fit to the fluorescence decay profiles and calculating the temperature

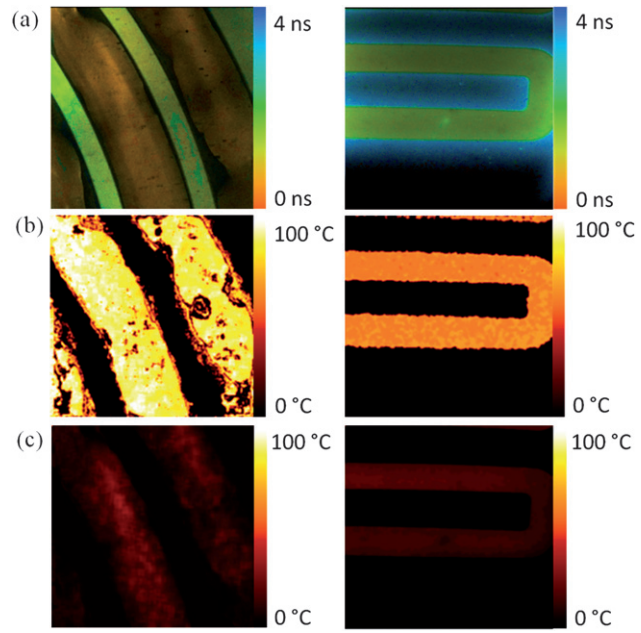

Fig. 3 Images of the device with droplets. (a) Average fluorescence lifetime maps calculated using a bi-exponential fit for the denaturation (left) and the annealing/extension (right) regions of the device. (b) Temperature maps calculated using the short lifetime component only, with mean values of 91.7 ± 8 °C (left) and 60.1 ± 4 °C (right). (c) Temperature maps calculated using a single exponential fit, with mean values of 10.5 ± 5 °C (left) and 14.1 ± 5 °C (right).

only from the shorter lifetime component data, we are able to remove the effect of the background signal (without use of any additional perturbations) and hence achieve an accurate measurement of fluidic temperature. If the same calculations had been performed using only the time-integrated intensity values, the background fluorescence contribution would lead to a lower value for the calculated temperature. For example, if only 5% of the collected photons originate from dye absorbed in PDMS, a measured temperature of 79 °C would result for a 'real' temperature of 95 °C, whilst for a 'real' temperature of 50 °C, a temperature of 46 °C would be calculated.

Concluding remarks

We have shown that by using FLIM it is possible to perform accurate temperature mapping of fluids within PDMS microfluidic devices by removing unwanted background signal (arising from dye absorbed in the PDMS substrate) through post-processing of the analytical signal. This background signal compromises time-integrated fluorescence measurements, and necessitates more complex approaches to calibration. Indeed, our approach is simple to implement and allows the straightforward analysis of multiple regions within a microfluidic device. Moreover, the acquisition times reported here could be significantly reduced by analysing the data with maximum likelihood estimator algorithms.[18]

We do note that the background signal is partially rejected by the sectioning strength of the confocal microscope, which can, in principle, be set to acquire fluorescence from only the central portion of a microchannel. However, such out-of-focus rejection is not complete and only reduces inversely with distance from the focal plane for a substrate volume with uniform dye absorption. Increasing the numerical aperture of the objective can increase background rejection significantly but would significantly limit the field of view and imaging depth, which is inconvenient when working with 200–500 μm wide channels and thick PDMS substrates. Crucially, the method described here does not require optically sectioned imaging and hence can be used with large fields of view and thick PDMS devices (5 mm thick devices were used herein). We also note that steady-state fluorescence polarisation anisotropy imaging using fluorescein has been recently demonstrated for temperature mapping.[19] While this approach also does not require a calibration curve (assuming a constant fluorescence lifetime), it may still suffer from significant background signals due to absorbed fluorescein. However, time-resolved fluorescence anisotropy imaging,[17] in principle, would require no calibration curve and could be used to remove the background signal by fitting a bi-exponential model to the anisotropy decay in a similar way to the work presented here.

Finally, although we have described a method for improving the accuracy of measuring fluidic temperatures when flowing rhodamine B solutions through PDMS channels, it should be noted that this technique can be applied more widely to a range of different substrate materials (and molecular fluorophores), and to a number of microfluidic applications that require 'background-free' fluorescence detection. On-chip drug screening assays,[20] for example, experience protein absorption that could lead to inaccurate measurement of kinetics and, whilst methods do exist to reduce protein absorption[21] the bi-exponential decay technique is likely to be more efficient.

Acknowledgements

T. Robinson would like to acknowledge a PhD studentship from the EPSRC through the Chemical Biology Centre of Imperial College. The authors would also like to acknowledge H.B. Manning for critical reading of the manuscript. The authors also acknowledge support by the RCUK Basic Technology Programme.

References

1 M. U. Kopp, A. J. Mello and A. Manz, *Science*, 1998, **280**, 1046–8.
2 S. Krishnadasan, J. Tovilla, R. Vilar, A. J. deMello and J. C. deMello, *J. Mater. Chem.*, 2004, **14**, 2655–2660.
3 S. R. Joung, C. J. Kang and Y. S. Kim, *Jpn. J. Appl. Phys.*, 2008, **47**, 1342–1345.
4 M. E. Lacey, A. G. Webb and J. V. Sweedler, *Anal. Chem.*, 2000, **72**, 4991–4998.
5 D. Ross, M. Gaitan and L. E. Locascio, *Anal. Chem.*, 2001, **73**, 4117–4123.
6 J. Kim, M. K. Chaudhury and M. J. Owen, *J. Colloid Interface Sci.*, 2000, **226**, 231–236.
7 J. Z. Kang, J. L. Yan, J. F. Liu, H. B. Qiu, X. B. Yin, X. R. Yang and E. K. Wang, *Talanta*, 2005, **66**, 1018–1024.
8 D. U. M. Kanai, S. Sugiura, Y. Shirasaki, J. S. Go, H. Nakanishi, T. Funatsu and S. Shoji, *μTAS 2003 International Conference on Miniaturized Chemical and Biochemical Analysis Systems*, 2003, **1**, 429–432.
9 N. R. Beer, E. K. Wheeler, L. Lee-Houghton, N. Watkins, S. Nasarabadi, N. Hebert, P. Leung, D. W. Arnold, C. G. Bailey and B. W. Colston, *Anal. Chem.*, 2008, **80**, 1854–1858.

10 Y. Schaerli and F. Hollfelder, *Mol. BioSyst.*, 2009, DOI: 10.1039/b907578j.
11 F. Courtois, L. F. Olguin, G. Whyte, A. B. Theberge, W. T. S. Huck, F. Hollfelder and C. Abell, *Anal. Chem.*, 2009, **81**, 3008–3016.
12 T. Glawdel, Z. Almutairi, S. Wang and C. Ren, *Lab Chip*, 2009, **9**, 171.
13 R. K. P. Benninger, Y. Koc, O. Hofmann, J. Requejo-Isidro, M. A. A. Neil, P. M. W. French and A. J. deMello, *Anal. Chem.*, 2006, **78**, 2272–2278.
14 Y. Schaerli, R. C. Wootton, T. Robinson, V. Stein, C. Dunsby, M. A. A. Neil, P. M. W. French, A. J. deMello, C. Abell and F. Hollfelder, *Anal. Chem.*, 2009, **81**, 302–306.
15 C. Dunsby, P. M. P. Lanigan, J. McGinty, D. S. Elson, J. Requejo-Isidro, I. Munro, N. Galletly, F. McCann, B. Treanor, B. Önfelt, D. M. Davis, M. A. A. Neil and P. M. W. French, *J. Phys. D: Appl. Phys.*, 2004, **37**, 3296.
16 N. P. Beard, C.-X. Zhang and A. J. deMello, *Electrophoresis*, 2003, **24**, 732.
17 J. R. Lakowicz, Principles of Fluorescence Spectroscopy, Springer, New York, 2006.
18 M. Kollner and J. Wolfrum, *Chem. Phys. Lett.*, 1992, **200**, 199–204.
19 G. Baffou, M. P. Kreuzer, F. Kulzer and R. Quidant, *Opt. Express*, 2009, **17**, 3291–3298.
20 S. Einav, D. Gerber, P. D. Bryson, E. H. Sklan, M. Elazar, S. J. Maerkl, J. S. Glenn and S. R. Quake, *Nat. Biotechnol.*, 2008, **26**, 1019–1027.
21 B. Huang, H. K. Wu, S. Kim and R. N. Zare, *Lab Chip*, 2005, **5**, 1005–1007.